INTERNATIONAL JOURNAL OF REFRIGERATION 60 (2015) 270–277

Available online at www.sciencedirect.com

ScienceDirect

journal homepage: www.elsevier.com/locate/ijrefrig

The effect of supercooling on ice structure in tuna meat observed by using X-ray computed tomography

Rika Kobayashi [a], *Norihito Kimizuka* [b], *Manabu Watanabe* [a], *Toru Suzuki* [a,*]

[a] *Department of Food Science and Technology, Graduate School of Tokyo University of Marine Science and Technology, 4-5-7 Konan, Minato-ku, Tokyo 108-8477, Japan*

[b] *School of Food, Agricultural and Environmental Sciences, Miyagi University, Taihaku-ku, Miyagi 982-0215, Japan*

ARTICLE INFO

Article history:
Received 9 March 2015
Received in revised form 8 July 2015
Accepted 10 July 2015
Available online 29 July 2015

Keywords:
Ice crystal
Supercooling
Freezing method
X-ray CT
Tuna meat

ABSTRACT

Several studies have reported that freezing a homogeneous food such as soy bean curd with deep supercooling (supercooled freezing) results in the formation of many particle ice and homogenous ice structure. However, ice crystal morphology may be affected by the cellular structure of the food. In this study, the ice crystal structure in tuna meat, a cellular food, frozen by the supercooled freezing method was investigated by X-ray computed tomography and compared with ice structures in tuna meat frozen by conventional freezing methods. The results showed that rod-like ice crystals grew parallel with the myofibers, and inhomogeneous ice structures formed in tuna meat frozen by the supercooled freezing method regardless of the degree of supercooling, in contrast to the ice structure in frozen soy bean curds. These ice crystals linked with each other to form rod-like ice structures due to mobility limitations imposed by the cellular structure.

L'effet de la surfusion sur la structure de la glace dans la viande de thon observé en utilisant la tomodensitométrie rayon-X

Mots clés : Cristaux de glace ; Surfusion ; Méthode de congélation ; CT rayon-X ; Viande de thon

* *Corresponding author.* Department of Food Science and Technology, Graduate School of Tokyo University of Marine Science and Technology, 4-5-7 Konan, Minato-ku, Tokyo 108-8477, Japan. Tel.: +81 3 5463 0585; Fax: +81 3 5463 0585.
E-mail address: toru@kaiyodai.ac.jp (T. Suzuki).

http://dx.doi.org/10.1016/j.ijrefrig.2015.07.011

Nomenclature

%	percent	1% = 1/100
°C	degree Celsius	0°C = 273 K
μm	micrometer	1 μm = 1×10^{-6} m
mm	millimeter	1 mm = 1×10^{-3} m
min	minute	1 minute = 60 seconds
Pa	pascal	1 Pa = 1 N/m^2
kV	kilo volt	1 kV = 1000 V
μA	micro ampere	1 μA = 1×10^{-6} A
h	hour	1 hour = 60 minutes
°C/h	degree Celsius per hour	rotational speed

1. Introduction

Freezing is one of the best methods for preserving food and extending its shelf life. However, food qualities such as texture, color, and water holding capacity decrease after freezing and thawing. Many factors contribute to this, one of which is mechanical stress due to volume changes caused by ice crystal formation. (Fennema, 1973). Therefore, the characteristics of the ice crystals, i.e., the size, shape and location of individual crystals, play dominant roles in changing the quality of frozen food and thus have been intensely studied in order to understand the mechanism of "crystallization" in food products. The size of ice crystals depends on the freezing rate (Bevilacqua and Zaritzky, 1980; Chevalier et al., 2000; Ngapo et al., 1999), and commercialized methods which freeze food rapidly have been developed. Methodologies that use factors other than freezing rate have also been developed to control the characteristics of ice crystals in food, such as pressure shift freezing, ultrasonic freezing, dehydrofreezing, and the use cryoprotectant such as sugar or antifreeze proteins (Sun and Zheng, 2006). Additionally, as demonstrated (Kobayashi et al., 2014a; Miyawaki et al., 1992; Simoyamada et al., 1999), freezing under conditions of deep supercooling results in the formation of spherical, homogenous fine ice crystals.

X-ray computed tomography has been widely used to measure the micro-structure of many food materials such as apples, bread and coffee beans (Frisullo et al., 2012; Mendoza et al., 2010; Van Dyck et al., 2014). Mousavi et al. (2007) used X-ray CT to measure the three-dimensional (3D) structure of ice crystals in frozen carrot, chicken and fish and showed that the size and shape of ice particles in frozen carrot and fish depended on the location of the ice in the tissue. However, the food materials used in that study were prepared using conventional freezing methods. To date, the effect of a supercooled freezing method on 3D ice particle structure has not been investigated. Therefore, we observed the 3D ice structure subjected to freezing under conditions of deep supercooling in soy bean curd using X-ray CT, and confirmed that the deeper the supercooling of soy bean curds, the more homogenous the ice crystals (Kobayashi et al., 2014b). Soy bean curd is homogenous, so ice crystal nucleation and growth should be isotropic and thus different from food materials containing cells, such as meat, fish, and vegetables; when these foods are frozen, the ice structure may be more complicated and anisotropic, due to water mobility being limited by the tissue structure as demonstrated (Ando et al., 2006, 2009). Thus it is unclear whether a supercooled freezing method results in the formation of a fine and homogenous ice structure in cell-based food materials.

In this study, a food material with a cellular structure was frozen using a supercooled freezing method and the ice particle structure was investigated by X-ray micro CT and compared with the ice structure formed using a conventional freezing method. Red tuna meat was used as it has previously been studied to determine the effect of refrigeration on the quality of the fish meat (Hagiwara et al., 2003; Viriyarattanasak et al., 2007).

2. Material and methods

2.1. *Sample preparation*

Two blocks (3–4 kg) of unfrozen tuna (*Thunnus orientalis*) dorsal red meat from fish caught off the Pacific Coast of Japan were purchased at the central market in Tsukiji, Japan. One block was used to compare the ice structure formed by supercooled freezing and conventional freezing methods and the other was used to examine the effect of the degree of supercooling on ice structure. Both tuna blocks were cut into 20 mm slabs, then into same-sized chunks, and cut into 20 mm cubes, as shown in Fig. 1. The cube samples were used that day. A thermocouple (Type-T, 0.046 mm diameter, T-T-40, Ishikawasangyo Co., Ltd., Japan) was inserted into the center of each tuna cube.

2.2. *Freezing method*

A liquid nitrogen programmable freezer designed by us was used for supercooled freezing. The samples were placed in the freezer chamber and frozen using the following program: the sample was kept at –5 °C for 1.5 h, the chamber temperature was dropped to –10 °C at a rate of –2 °C/h. During this cooling process, some samples took the supercooling state and reached subsequently released supercooling state spontaneously. After the releasing of supercooling state, a set temperature of chamber temperature was changed immediately to –75 °C at a rate of –252 °C/h.

Conventional rapidly frozen samples were produced by freezing tuna cubes in an air blast freezer (Test machine, manufactured by Mayekawa Mfg. Co., Ltd., Japan) at –40 °C and an air flow of 2.0 m/s. Conventional slow freezing was performed in an incubator (FMU-1331, Fukushima Industries Corporation. Japan) at –15 °C in static air. The temperature of each tuna sample was recorded during each of the three freezing processes and a real time freezing curve was constructed using a data logger (THERMODAC 5001A, Eto-denki Co. Ltd., Japan). After freezing, all samples were stored in a –80 °C chest freezer (MDF-192, Sanyo Electric Co., Ltd., Japan) for up to 2 days before freeze-drying.

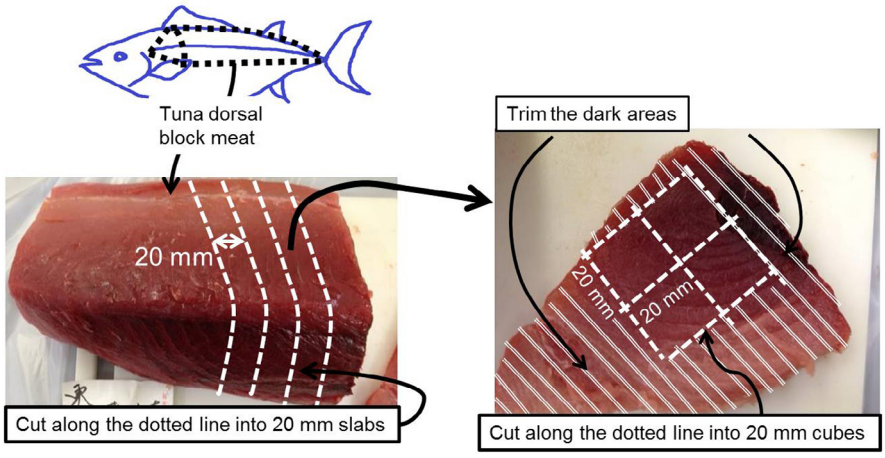

Fig. 1 – How to prepare the tuna cube samples from tuna dorsal red meat.

2.3. *Measurement of ice structure by X-ray CT*

Ice crystal structures in frozen tuna sample were observed using X-ray CT (Sky scan 1172, Bruker microCT, Belgium) following the method as demonstrated (Mousavi et al., 2005). Frozen tuna cubes were dried for 1 week in a freeze-drier (Kyowac RLE-52, Kyowa Vacuum Engineering. Co., Ltd., Japan) at approximately 5 Pa and between –40 °C and +5 °C to sublimate the ice crystals in frozen tuna meat. Dried tuna cubes were cut into rectangular parallelepiped shapes 5 mm long and wide and 10 mm high. The myofibers were parallel to the length direction. The samples were placed on the metal sample stage and scanned by the CT scanner with the source power set at 49 kV and 100 μA. The tuna meat samples for comparing ice structure formed by different freezing methods were rotated 180° at 0.2° steps and transmission images were obtained using a CCD camera with a 4.9 μm image pixel size. Other samples which is for examining the effect of the degree of supercooling on ice structure were scanned with rotating 180° at 0.4° steps and transmission images were obtained using a CCD camera with a 7.75 μm image pixel size.

After scanning, cross sectional images of all tuna meat sample were reconstructed using reconstruction software (NRecon Skyscan) by generating 256-grayscale cross sectional images by limiting the linear attenuation range to 0–0.04. Accumulation of tomograms provided the 3D structure of the ice crystals following image processing (CTVox, Skyscan). The cross sectional images, which were 8 bit-gray scale bitmap images, were converted into binary images with a set threshold value of 180. Each ice crystal area and diameter was calculated using image-analysis software (WinRoof, Mitani Co., Ltd., Japan).

3. Results and discussion

Fig. 2 shows the freezing curves of tuna meat frozen by three freezing methods: airblast freezing, slow freezing, and supercooled freezing. The supercooled freezing curve shows a sudden temperature increase due to release of supercooled water whereas the freezing curves generated by the conventional methods, airblast and slow freezing showed a typical plateau at the equilibrium freezing temperature (–1.8 °C). This supercooled freezing method resulted in ice nucleation, i.e., release of supercooled water at –7.1 °C. The degree of supercooling, which is the difference between the supercooling release temperature and the equilibrium freezing temperature, is 5.3 °C (7.1–1.8).

The airblast freezing curve shows an increase in temperature around –40 °C due to sample operation, namely, moving the frozen sample from the –40 °C airblast freezer to the –80 °C chest freezer, and thus can be disregarded.

Tomograms of tuna meat frozen by the different freezing methods are showed in Figs. 3 and 4. Fig. 3 shows cross sectional views of the myofibers and Fig. 4 shows views parallel to the myofibers. The white areas correspond to ice crystals and the black areas to tissues. Enlarged images of Fig. 3 or 4 (original) (i), (ii) and (iii) are shown in Fig. 3 or 4 (enlarged) (i), (ii) and (iii). As can be seen in the cross sectional images (Fig. 3, original), ice crystals in tuna meat subjected to slow freezing (ii) were large and rod-like whereas ice crystals formed by

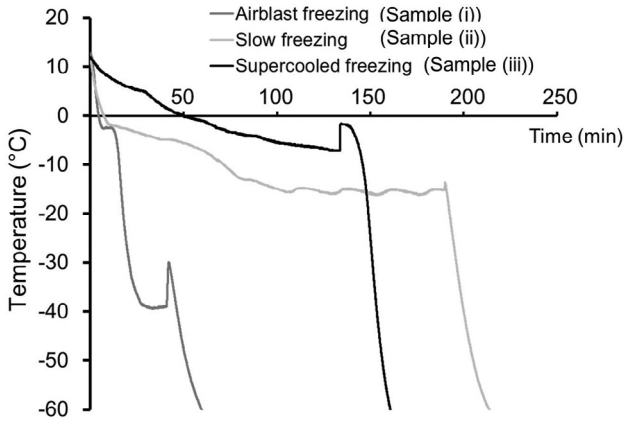

Fig. 2 – Freezing curves of tuna meat frozen by three freezing methods.

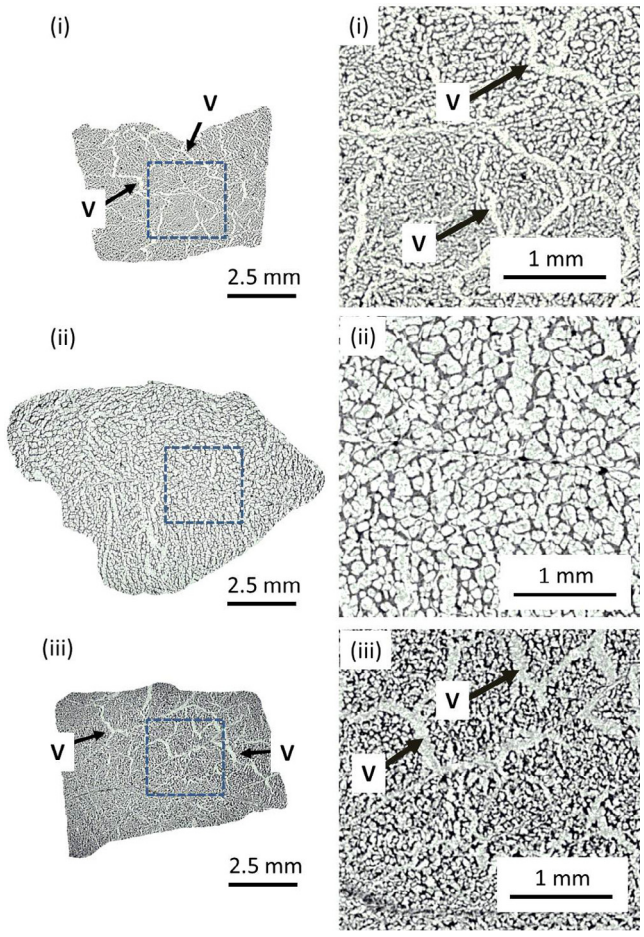

Fig. 3 – Images cross-sectional to myofibers in tuna meat frozen by three freezing methods: (i) conventional rapid freezing (airblast freezing method), (ii) conventional slow freezing, (iii) supercooled freezing method. Images on the left are the original and enlarged images are shown on the right.

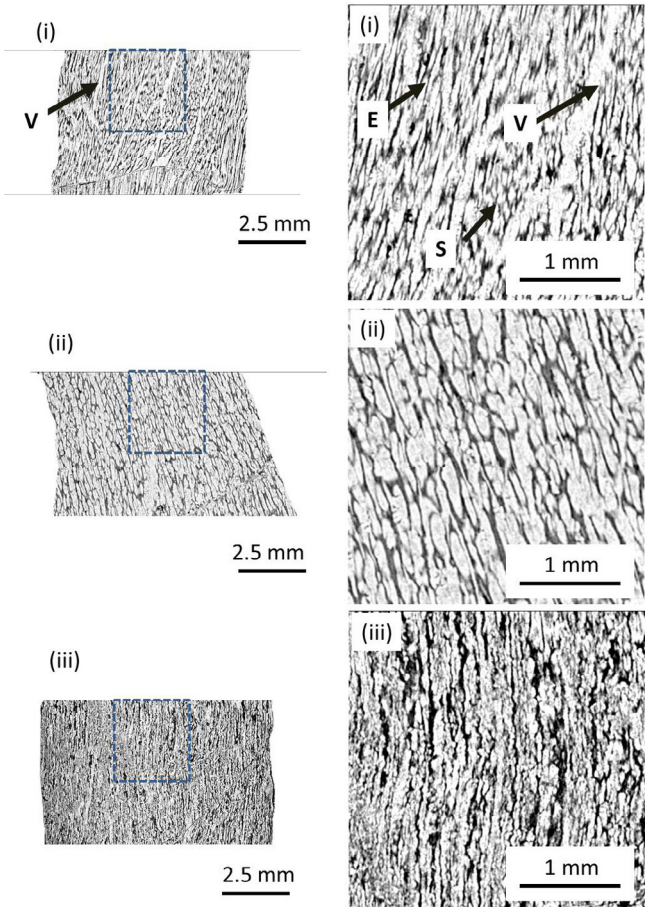

Fig. 4 – Images parallel to myofibers of tuna meat frozen by three freezing methods: (i) conventional rapid freezing (airblast freezing method), (ii) conventional slow freezing, (iii) supercooled freezing method. Images on the left are the original and enlarged images are shown on the right.

airblast freezing (i) and by supercooled freezing (iii) were individual particles. These characteristics were independent of location in the cross sectional images.

Although some voids like cracks were seen apparently in Fig. 3(i) and (iii) (indicated by the arrows with "V"), from enlarging figure, it was realized in Fig. 3 (enlarged) that the void-like cracks were not generated during freeze-drying but rather are due to ice crystal growth between the muscle bundles: the muscle bundle is an aggregate of myofibers, and diameters of myofibers are around 50–100 μm, as shown by Nakamura et al. (2005). Fig. 4 (original) indicates that ice crystals in each parallel section tend to grow along the myofiber and form elongated structures. Ice crystals in samples frozen using the slow freezing method are oval whereas the ice crystals in tuna meat subjected to air blast freezing show a complex structure of many small specular ice crystals (indicated by the arrows with "S" in Fig. 4 (enlarged) (i)) mixed with elongated ice crystals (indicated by the arrows with "E" in Fig. 4 (enlarged) (i)). The void like cracks were also shown in Fig. 4 (original and enlarged) (i) (indicated by the arrows with "V"). The ice crystals in the samples frozen by supercooled freezing are finer than those generated by the other two methods but the detailed morphology of the ice crystals is not evident from this figure. The images were enlarged to better visualize the ice crystals and are shown in Fig. 4 (enlarged) (i), (ii) and (iii). Ice crystals in samples frozen by airblast and supercooled freezing were overall rod-like but their detailed structures were different. In the airblast frozen samples the rod-like ice crystals appeared to be formed by the growth of individual ice crystals (Fig. 4 (enlarged) (i)) whereas the ice crystals in the supercooled frozen samples (Fig. 4 (enlarged) (iii)) were apparently formed by the linear connection of many fine ice crystals along the myofiber upon supercooling release of water.

The tomograms shown in Fig. 3 and Fig. 4 show arbitrary positions in the samples and thus may not reflect the ice crystal structure at specific positions in the sample. To address this, 3D images of tuna meat frozen by the three freezing methods are shown in Fig. 5, which shows a 3 mm × 4 mm × 4 mm section of each sample. Void parts in the images show the ice crystal structure and the bright parts show the solid tuna meat. The 3D images show little local difference in the ice structure in each sample. Therefore, the structural information

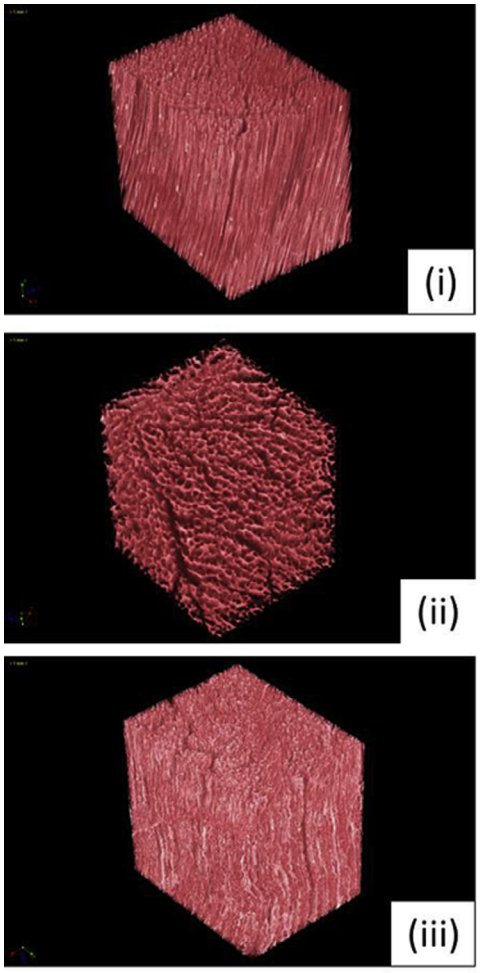

Fig. 5 – 3D images of tuna meat frozen by three freezing methods: (i) conventional rapid freezing method (airblast freezing method), (ii) conventional slow freezing method, (iii) supercooled freezing method.

provided by the tomograms (Figs. 3 and 4) represent the overall ice crystal structure at any position in the respective sample.

Next, the effect of the degree of supercooling on the ice structure in frozen tuna meat was investigated. Fig. 6 shows the freezing curves for tuna meat frozen at different degrees of supercooling. There is a sudden temperature increase due to the release of supercooled water in the curves for samples (iv) and (v). For sample (iv), ice nucleation, i.e., the release of supercooled water, occurred at –3.7 °C, and at –6.2 °C for sample (v). The plateau in the curve for both samples showed that the equilibrium freezing temperature was –1.8 °C. Therefore, the degree of supercooling was 1.9 °C for sample (iv) and 4.4 °C for sample (v).

Figs. 7 and 8 show the tomograms for tuna meat frozen with different degrees of supercooling (samples (iv) and (v), respectively). Fig. 7 shows a cross sectional view and Fig. 8 shows the view parallel to the myofibers. As with Figs. 3 and 4, details regarding the ice morphology were not evident from the original scale images and so a section of each image was enlarged, as also shown in Figs. 7 and 8.

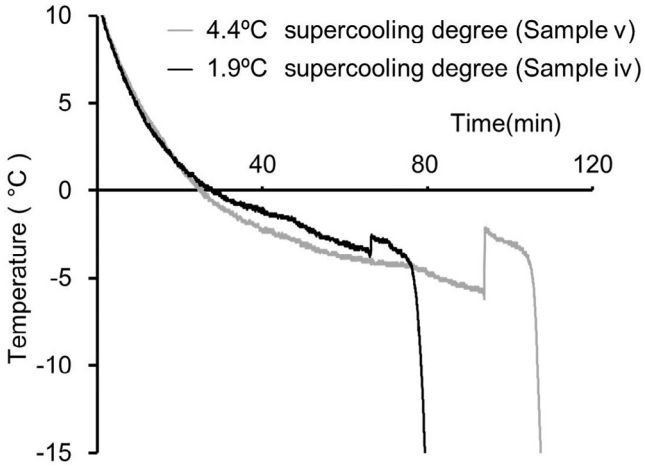

Fig. 6 – Freezing curves of tuna meat frozen by the supercooled freezing method with different degrees of supercooling.

Fig. 7 shows fine ice crystals in both samples (iv) and (v) but of different shapes: the ice crystals in the cross sectional view of sample (iv), subjected to a smaller degree of supercooling, have various shapes such as round, elongated and tube-like, whereas sample (v), subjected to larger degree of supercooling, showed polygonal-shaped crystals.

Ice crystals between the muscle bundles, visible in Fig. 3 (enlarged) (ii), (iii) could not be seen in Fig. 7. There are some reports that the freshness affects ice structure. Love (1968) reported that the ice crystals in pre-rigor cod muscle and post-rigor cod muscle differed both in the quantity of extracellular ice and the shapes of the intracellular ice crystals. Kaale et al. (2013) also reported that the freshness of fish meat, pre-rigor or post-rigor, affects the morphology of ice formed during the superchilling process. Therefore, ice crystals growing between

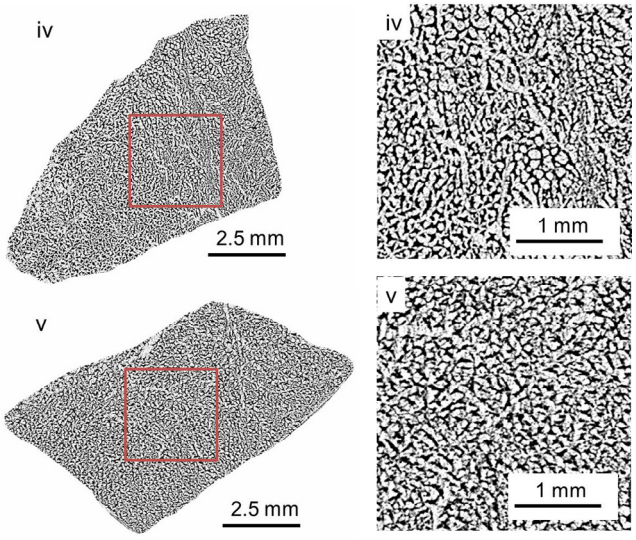

Fig. 7 – Images cross-sectional to myofibers of tuna meat frozen by the supercooled freezing method with different degrees of supercooling; (iv) 1.9 °C of supercooling, (v) 4.4 °C of supercooling.

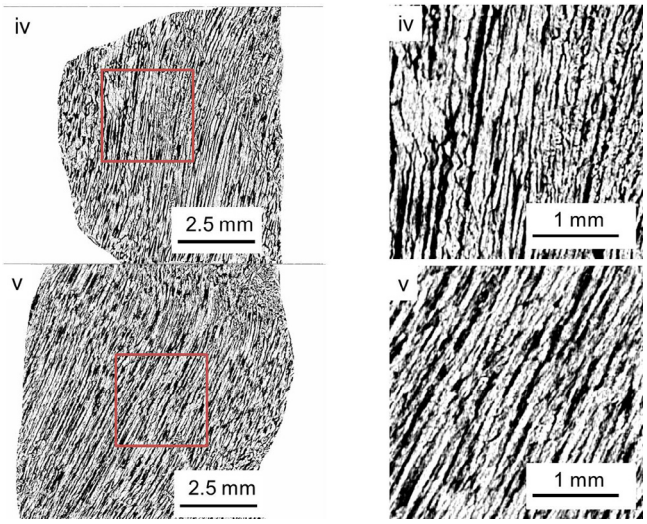

Fig. 8 – Images taken parallel to the myofibers in tuna meat frozen by the supercooled freezing method using different degrees of supercooling: (iv) 1.9 °C of supercooling, (v) 4.4 °C of supercooling.

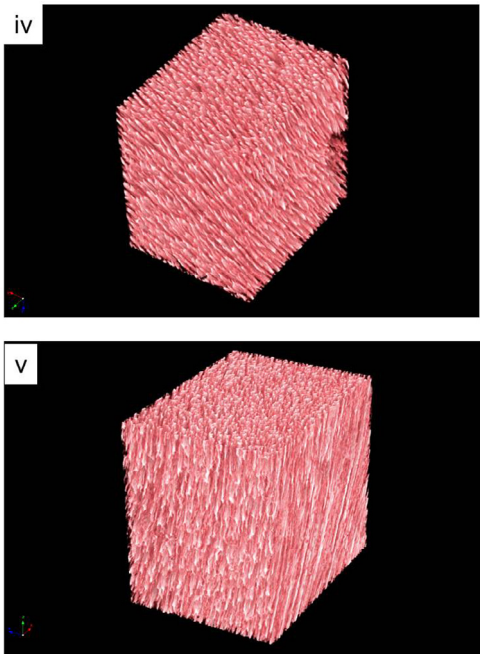

Fig. 10 – 3D images of tuna meat frozen by the supercooled freezing method with different degrees of supercooling; (iv) 1.9 °C supercooling, (v) 4.4 °C supercooling.

the muscle bundles in tuna meat may not depend on the freezing process but on the freshness. Thus, the difference of the images shown in Fig. 7 and in Fig. 3 may be attributed by the difference of freshness, since tuna meat blocks which were provided to image of Fig. 7 and Fig. 3 were different, though these freshness were not defined.

Fig. 8 shows sectional images parallel to the muscle bundles of tuna meat frozen with different degrees of supercooling. Although the ice crystals in sample (iv) and sample (v) showed rod-like forms, the rod-like ice crystals appeared to be formed by the linear connection of many small ice crystals, as described in Fig. 4. Furthermore, the diameter of the rod-like ice crystals in sample (iv) was larger than in sample (v). Fig. 9 shows the size distribution of ice crystal particles from the cross-sectional images in Fig. 7, and thus the diameter of the rod-like ice crystals.

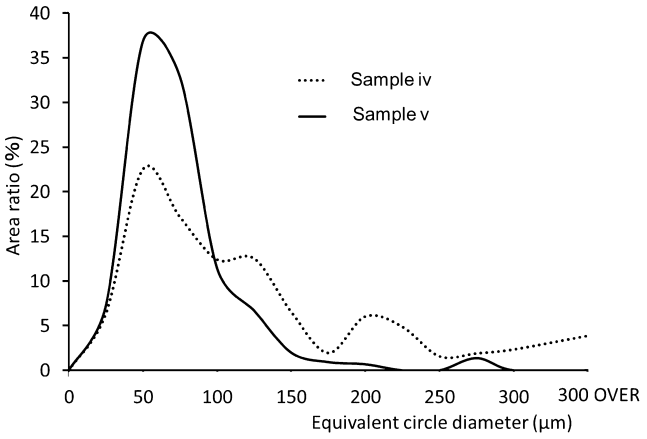

Fig. 9 – Size distribution of ice crystals in tuna meat frozen by the supercooled freezing method using different degrees of supercooling: (iv) 1.9 °C of supercooling, (v) 4.4 °C of supercooling.

Sample (v) shows one peak distribution of ice particle size ranged from 25 to 100 μm while the size distribution for sample (iv) spread over a wide range and distributed into three peaks, showing quantitatively that a larger degree of supercooling induces the formation of homogenous, thin ice crystals.

3D images of tuna meat frozen using different degrees of supercooling are shown in Fig. 10. The ice crystal structures observed in the 3D images are similar to those observed in the tomograms (Figs. 7 and 8), confirming that the structures of ice crystals in both samples are independent of the local position visualized by the tomogram and are universal characteristics, thus establishing that the results from tomograms are representative of any location in the sample.

There is anisotropic ice crystals in tuna meat regardless of the freezing method used. Several previous studies focused on the 3D structure of ice crystals in food materials with cellular structures; for example, Ishiguro and Horimizu (2008) used confocal laser scanning microscopy and reported that the ice crystals grew along the myofibers and formed rod-like shapes in chicken meat, supporting our results. Mousavi et al. investigated ice crystal formation in frozen foods such as carrot and salmon using X-ray CT and reported that ice crystals in carrot had different shapes depending on the local tissue structure, but did not discuss why frozen salmon had a rod-like ice structure. Do et al. (2004) have also reported rod-shaped ice crystals in frozen beef by 3D observation using a micro-slicer image processing system but did not discuss the underlying mechanism.

On the other hands, it was generally known that the ice structures in frozen food are affected by local freezing rate as well as by cell structure. In our study, the samples were

prepared to be small pieces as 20 mm cubes as mentioned in Section 2, so that it was considered the difference of local freezing rate was little in sample tuna meat. Therefore, it was proved that the rod-like ice crystals observed in our result were mainly affected by cell structure of tuna meat especially muscle tissue, even if in the supercooled freezing method. Ice crystal formation in food materials with and without cellular structures differs greatly. For example, soy bean curds have no cellular structure and small, spherical, homogenous ice particles form when frozen using the supercooled freezing method but are affected by the degree of supercooling (Kobayashi et al., 2014b). In contrast, tuna meat frozen by the supercooled freezing method formed inhomogeneous ice structures at any degree of supercooling. Closer examination (Figs. 3 and 4 (enlarged) (iii)) revealed fine ice crystals linearly connected parallel to the myofibers of tuna meat frozen by the supercooled freezing method. Thus, the ice nucleation process in tuna meat frozen by the supercooled freezing method is the same as that in soy bean curd. However, ice growth following ice nucleation was different between the two food materials because ice crystal growth perpendicular to myofibers would be restricted by the low water permeability of the cell membranes in tuna meat. A larger degree of supercooling in tuna meat than in this study may result in homogenous ice structure as in soy bean curds. However, the freshness of the tuna meat affected ice crystal structure even when using the supercooled freezing method. The interactions between water and solids in raw food materials such as fish, meat and vegetables are changed by the biological condition of the material, such as its freshness, resulting in changes in the nucleation and growth of ice crystals. Sanguansri and Nutsuda (2010) has reported that ice crystals formed in starch gels subjected to the supercooled freezing method were inhomogeneous in structure and this was explained as follows: starch gels retrogradation as they were cooled slowly during the freezing process to obtain the supercooled state, causing an inhomogeneous distribution of water in the starch gels and subsequent formation of ice crystals with various sizes and shapes.

4. Conclusion

In this study, we used X-ray computed tomography to investigate how ice structures in cellular food tissue, such as tuna meat, formed by the supercooled freezing method compared with those formed in conventional freezing methods and to those formed during supercooled freezing of homogeneous foods such as soy bean curds. The results revealed that tuna meat frozen by the supercooled freezing method had a similar ice structure by conventional freezing method. Specifically, they had rod-like ice crystals aligned parallel to the myofibers, and inhomogeneous and anisotropic ice structures, in contrast to the ice structure in frozen soy bean curds, and the diameter of rod-like ice crystals depended on degree of supercooling.

Furthermore, it was found that these ice crystals linked with each other to form rod-like ice structures. These characteristics of ice structure are attributable to the limited water mobility imposed by the cellular structure, which would be affected by freshness.

Therefore, the supercooled freezing method has potential for improving the quality of frozen food by controlling the ice crystal structure but the condition of the food materials, such as freshness, must be controlled. Additionally, to attain a larger degree of supercooling, innovative methodologies such as the use of high pressure are required. In order to utilize the supercooled freezing method effectively, not only ice nucleation but also the growth behavior of ice crystals after nucleation, and the effect of water distribution and mobility in food materials, need to be understood in detail.

Acknowledgments

This work was partly supported by the Japan Science and Technology Agency and the Ministry of Education, Culture, Sports, Science, and Technology of Japan “MEXT Revitalization Project for the creation of Fisheries Research and Education Center in Sanriku”.

REFERENCES

Ando, H., Fukuoka, M., Miyawaki, O., Suzuki, T., 2006. Damage evaluation on freeze-thawing process of food by using NMR. Trans. JSRAE 23, 305–312 (in Japanese).

Ando, H., Fukuoka, M., Miyawaki, O., Watanabe, M., Suzuki, T., 2009. PFG-NMR study for evaluation of freezing damage in onion tissue. Biosci. Biotechnol. Biochem. 73, 1257–1261.

Bevilacqua, A.E., Zaritzky, N.E., 1980. Ice morphology in frozen beef. Int. J. Food Sci. Technol. 15, 589–597.

Chevalier, D., Le Bail, A., Ghoul, M., 2000. Freezing and ice crystals formed in a cylindrical food model: part 1. Freezing at atmospheric pressure. J. Food Eng. 46, 277–285.

Do, G.S., Sagara, Y., Tabata, M., Kudoh, K., Higuchi, T., 2004. Three-dimensional measurement of ice crystals in frozen beef with a micro-slicer image processing system. Int. J. Refrigeration 27, 184–190.

Fennema, O.R., 1973. Nature of the freezing process. In: Fennema, O.R., Powrie, W.D., Marth, E.H. (Eds.), Low-Temperature Preservation Foods and Living Matter. Marcel Dekker Inc, New York, pp. 151–227.

Frisullo, P., Barnabà, M., Navarini, L., Del Nobile, M.A., 2012. Coffee arabica beans microstructural changes induced by roasting: An X-ray microtomographic investigation. J. Food Eng. 108, 232–237.

Hagiwara, T., Hayashi, R., Suzuki, T., Takai, R., 2003. Fractal analysis of ice crystals in frozen fish meat. Jpn J. Food Eng. 4, 11–16.

Ishiguro, H., Horimizu, T., 2008. Three-dimensional microscopic freezing and thawing behavior of biological tissues revealed by real-time imaging using confocal laser scanning microscopy. Int. J. Heat Mass Transf. 51, 5642–5649.

Kaale, L.D., Eikevik, T.M., Rustad, T., Nordtvedt, T.S., Bardal, T., Kjørsvik, E., 2013. Ice crystal development in pre-rigor Atlantic salmon fillets during superchilling process and following storage. Food Control 31, 491–498.

Kobayashi, R., Kanesaka, N., Watanabe, M., Suzuki, T., 2014a. Effect of the breaking temperature of supercooling on ice characteristics and drip loss of foods in supercooled freezing method. Trans. JSRAE 31, 297–303 (in Japanese).

Kobayashi, R., Kimizuka, N., Suzuki, T., Watanabe, M., 2014b. Effect of supercooled freezing methods on ice structure observed by X-ray CT. Proceedings of 3rd IIR International

Conference on Sustainability and the Cold Chain, London, UK. 174 of Reference number.
Love, R.M., 1968. Ice formation in frozen muscle. In: Hawthorn, J., Rolfe, E.J. (Eds.), Low Temperature Biology of Foodstuffs. Pergamon Press, London, pp. 105–124.
Mendoza, F., Verboven, P., Tri Ho, Q., Kerckhofs, G., Wevers, M., Nicolaï, B., 2010. Multifractal properties of pore-size distribution in apple tissue using X-ray imaging. J. Food Eng. 99 (2), 206–215.
Miyawaki, O., Abe, T., Yano, T., 1992. Freezing and Ice structure formed in protein gels. Biosci. Biotechnol. Biochem. 56, 953–957.
Mousavi, R., Miri, T., Cox, P.W., Fryer, P.J., 2005. A novel technique for ice crystal visualization in frozen solids using X-ray micro-computed tomography. J. Food Sci. 70, e437–e442.
Mousavi, R., Miri, T., Cox, P.W., Fryer, P.J., 2007. Imaging food freezing using X-ray microtomography. Int. J. Food Sci. Technol. 42, 714–727.
Nakamura, Y., Ando, M., Seoka, M., Kawasaki, K., Tsukamasa, Y., 2005. Comparison of the proximate compositions, breaking strength and histological structure by the muscle positions of the full-cycle cultured Pacific bluefin tuna Thunnus orientalis. Fish Sci. 71, 605–611.
Ngapo, T.M., Babare, I.H., Reynolds, J., Mawson, R.F., 1999. Freezing rate and frozen storage effects on the ultrastructure of samples of pork. Meat Sci. 53, 159–168.
Sanguansri, C., Nutsuda, P., 2010. Undercooling associated with slow freezing and its influence on the microstructure and properties of rice starch gels. J. Food Eng. 100, 310–314.
Simoyamada, M., Tomatsu, K., Watanabe, K., 1999. Effect of precooling step on formation of soymilk freeze-gel. Food Sci. Technol. Res. 5, 284–288.
Sun, D., Zheng, L., 2006. Innovations in freezing process. In: Sun, D.-W. (Ed.), Handbook of Frozen Food Processing and Packaging. CRC Press, Florida, pp. 175–192.
Van Dyck, T., Verboven, P., Herremans, E., Defraeye, T., Van Campenhout, L., Wevers, M., et al., 2014. Characterisation of structural patterns in bread as evaluated by X-ray computed tomography. J. Food Eng. 123, 67–77.
Viriyarattanasak, C., Watanabe, M., Suzuki, T., 2007. Analysis of metmyoglobin formation rates in frozen tuna meat during low temperature storage. Trans. JSRAE 24, 227–233.